

Influence of Air and Nitrogen Atmosphere on g-C₃N₄ Synthesized from Urea

Atita Tapo¹, Pornapa Sujaridworakun¹, Wasana Khongwong², Piyalak Ngerchuklin² and Chumphol Busabok^{2,*}

¹Department of Materials science, Faculty of Science, Chulalongkorn University, Bangkok, 10330, Thailand

²Expert Centre of Innovative Materials, Thailand Institute of Scientific and Technological Research, Pathum Thani 12120, Thailand

Received: 29 April 2022, Revised: 12 June 2022, Accepted: 26 June 2022

Abstract

This work attempted to develop g-C₃N₄ synthesized from urea using for photocatalysis application under visible light. The effects of the heat treatment parameters such as reaction temperatures (450, 500, 550, and 600°C) and controlled atmospheres during synthesis (ambient air and nitrogen) were studied. Urea powders were placed in an alumina boat crucible and put in a tube furnace and then heated up from ambient temperature to 250°C with a heating rate of 10°C/min for 10 min soaking. After that, the temperature was decreased to 220°C and soaked for 10 min followed by increasing the temperature to 450°C-600°C with 2°C/min and soaked for 30 min in ambient air or nitrogen atmosphere. The synthesized powders were characterized for morphology by SEM, phase analysis by XRD, and light absorption by UV-VIS-NIR spectrometer. The photocatalytic properties of synthesized g-C₃N₄ in ambient air or nitrogen atmosphere were investigated via the degradation of methylene blue under visible light irradiation (more than 450 nm wavelength generated from 50W LED lamp). The yield of products synthesized in the N₂ atmosphere was higher than in the ambient air due to less decomposition of urea compared to the ambient air. The band gap energy of g-C₃N₄ synthesized in N₂ was narrower than that synthesized in the ambient air resulting in a wider wavelength absorbed. Moreover, the increasing temperatures lead to reducing of band gap energy of g-C₃N₄ in the N₂ atmosphere.

Keywords: Visible light, Photocatalysis, g-C₃N₄; Ambient air, Nitrogen atmosphere

1. Introduction

Photocatalyst materials are semiconductor materials such as TiO₂, SrTiO₃, CdS, BiVO₄, Ta₃N₅, TaON, g-C₃N₄, Ag₃PO₄, and their nanostructured have gotten attention in use as photocatalyst material which use light to activate a chemical reaction [1]. Recently, many researchers have studied photocatalyst materials for harvesting a range spectrum of sunlight for the reaction. The sunlight energy spectrum are composed of 5% UV-A rays (321-400 nm), 39% - 45% visible light (400-700 nm) and 40% are infrared (700-1,440 nm) [2]. The property requirements of such photocatalyst materials are high visible-light quantum efficiency, stability, safety, and cheapness. Among semiconductor materials, graphitic carbon nitride (g-C₃N₄) has a lot of attention because of its metal-free polymeric, low cost, chemical stability, and non-toxic performance. Its narrow band gap energy of 2.7 eV can absorb visible light. While g-C₃N₄ has a suitable property for photocatalyst, it still has problems of low photocatalytic efficiency due to a small surface area with limited active sites, a high charge recombination rate, and the ability to harvest visible light are low [3]. To enhance the photocatalytic efficiency of g-C₃N₄ photocatalysts, there is a design

strategy to solve problems to get highly efficient photocatalytic such as band gap engineering, defect control, pore texture tailoring, dimensionality tuning, surface sensitization, heterojunction construction, co-catalyst loading and nanocarbon loading [1]. One of all design strategies, defect control has been widely studied and results were accepted from a high degree of crystallinity resulting in improvement of photocatalytic redox reactions [4]. In addition, a recent defect control study was to demonstrate the creation of defect structures such as nitrogen vacancies [5] and amorphous [6] which could improve the visible light activity. For example, in the fabrication of the amorphous g-C₃N₄ at 620 °C in an argon atmosphere, the results showed an amorphous structure that could narrow the bandgap from 2.7 to 1.9 eV. Moreover, heat treatment at high temperature in an argon atmosphere, in H₂, NH₃ [7], [8], or vacuum atmosphere could generate nitrogen or carbon vacancies [1]. Furthermore, some studies were conducted for different synthesis conditions in ambient air, H₂, NH₃, N₂, and Argon with the use of precursors including melamine, and dicyandiamide by equimolar ratio, and the obtained result showed that the gas atmosphere had an impact on the photocatalytic activity [9].

By the way, g-C₃N₄ was synthesized with many precursors such as urea [10], thiourea, melamine [9], dicyandiamide [6], cyanamide, and guanidine hydrochloride by a simple process in synthesis [11], [12]. Urea is a common raw material in the industry or readily available raw material because urea has been used as raw material for producing many chemicals such as biuret and melamine on an industry scale [10]. Urea has suitable for precursors used to produce g-C₃N₄ because many precursors are difficult to access, some are unstable and some are highly explosive and urea is considered inexpensive. Previously, synthesized g-C₃N₄ from different precursors between urea and melamine showed that g-C₃N₄ synthesized from urea had a high BET surface area or larger surface areas than one synthesized from melamine [12].

Therefore, this work had attempted to develop g-C₃N₄ by thermal decomposition of urea used as a precursor and investigated the effects brought by different temperatures and atmospheres (ambient air and nitrogen) on the products.

2. Experimental

2.1 Synthesis of g-C₃N₄

g-C₃N₄ was prepared in a tube furnace. Urea (Kemaus (Australia), purity of 99.0-100.5%) was used as a precursor. The precursor was put in an alumina boat and then placed into the center of the tube furnace. The powders were heated up from ambient temperature to 250°C with a heating rate of 10°C/min for 10 min. After that, the temperature was decreased to 220°C and soaked for 10 min followed by increasing the temperature to 450°C-600°C with 2°C/min and soaked for 30 min in ambient air or nitrogen atmosphere.

2.2 Characterization

The synthesized powders were characterized by an X-ray diffractometer (XRD, 6000, Shimadzu Corporation, Japan) for monochromatized CuK_α ($\lambda = 1.5406 \text{ \AA}$) radiation. The interlayer distance of the layers was calculated using Bragg's law equation Eq.(1)

$$2d\sin\theta = n\lambda \quad (1)$$

where d is the interlayer distance (\AA), θ is Bragg's angle (at $2\theta = 27^\circ$), n is the diffraction order, and λ is the wavelength of the incident beam (\AA).

The numbers of layers were determined by using the Debye-Scherrer Eq. (2) and (3) [13]:

$$t = (0.89\lambda)/(\beta\cos\theta) \quad (2)$$

$$n = t/d \quad (3)$$

where t is the thickness, β is the full width at half maximum (FWHM) position of (002), n is the number of graphene layers, and d is the interlayer distance position of (002) at $2\theta = 27^\circ$. The morphology of the synthesized powders was studied by using a scanning electron microscope (SEM) (FESEM, JSM-6304F, JEOL, Japan), specific surface area using a BET surface area analysis (Quantachrome instruments version 3.01), and light absorption by UV-VIS-NIR spectrometer (Avalight-DH-S version 1.3, AvaSpec-ULS2048L, AVANTES, Netherland).

2.3 Photocatalytic tests

The photocatalytic properties of synthesized g-C₃N₄ in ambient air or nitrogen atmosphere were investigated via the degradation of methylene blue (MB) under visible light irradiation (wavelength of more than 450 nm, generated from a 50W LED lamp). In the first step, methylene blue solution was prepared at 120 mL with a concentration of 10 ppm and then mixed with 50 mg of the synthesized powders. In the second step, the suspensions were magnetically stirred for 2 h in the dark surrounding. Finally, the suspensions were irradiated for 7 h in visible light to test the photocatalytic efficiency. For all tests, the samples were taken every 1 h. The concentration of methylene blue was analyzed by recording the absorption intensity from a UV-VIS-NIR spectrometer.

3. Results and discussion

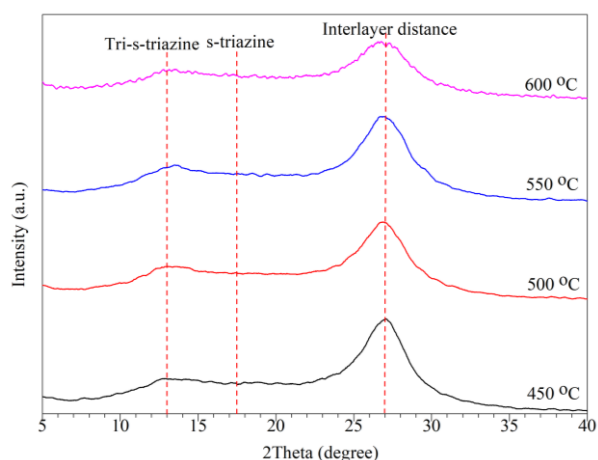
3.1 XRD analysis

The XRD patterns of g-C₃N₄ synthesized in ambient air and nitrogen atmosphere at 450°C-600°C are shown in Fig. 1. It was demonstrated that all samples consist of two obvious peaks at about 13° (Tri-s-triazine) and 27°, corresponding to the g-C₃N₄ [14]. In the ambient air atmosphere, with increasing temperature, the high-angle peak (approximate at 27°) tended to be sharper due to condensation to obtain a good adjustment of the aromatic planes [12]. On the other hand, the high-angle peak (approximate at 27°) tended to be broader as increasing temperature from 450°C to 600°C in a nitrogen atmosphere. These showed that crystalline size was small with increasing temperature. Furthermore, urea was used as a precursor for synthesized g-C₃N₄ so it did not show an s-triazine peak (approximate at 1°) in Fig. 1, and other intermediates form due to pyrolysis of urea that is ill-connected heptazine-based g-C₃N₄ [12]. Table 1 shows the crystal size in the nitrogen atmosphere. It is found that a broad peak is affected by a small crystal size as the main constituent. As the temperature increases, smaller crystal size is obtained. Previous research had studied pyrolysis using various inert gases [6], [9] and found nitrogen or carbon vacancies defect in structure g-C₃N₄. Nitrogen-vacancy defects provided the potential to considerably expand the visible light absorption spectrum while also suppressing unexpectedly rapid recombination [1].

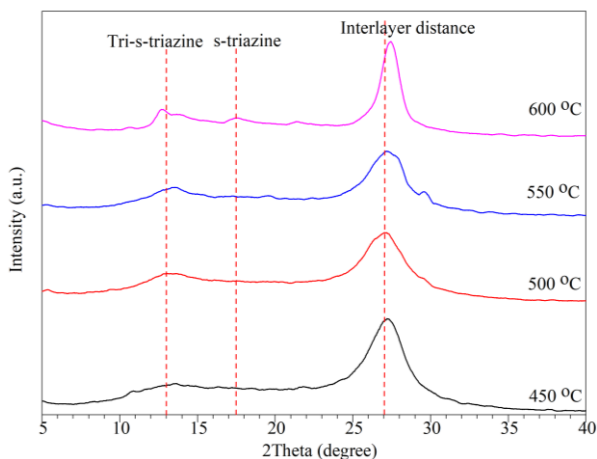
The interlayer distances (d_{002}) of samples were varied between 0.8-0.9 Å as shown in Table 1, calculated from the full width at half maximum and the position of (002) reflection at $2\theta = 27^\circ$. Furthermore, as pyrolysis temperature increased, a peak at 13° became more obviously observed. This is the fact that higher temperature allows greater plane organization and more connection of g-C₃N₄ structure motifs, resulting in a larger planar size [12].

Table 1. The interlayer distances (d_{002}) and mean thickness of graphitic stack-based $g-C_3N_4$

| $g-C_3N_4$ | d_{002} (Å) | Mean thickness of stacks (nm) | No. layers |
|---------------------|---------------|-------------------------------|------------|
| Ambient air - 450°C | 0.902 | 3.00 | 33 |
| Ambient air - 500°C | 0.907 | 2.70 | 28 |
| Ambient air - 550°C | 0.858 | 2.97 | 34 |
| Ambient air - 600°C | 0.839 | 5.52 | 65 |
| Nitrogen - 450°C | 0.932 | 2.64 | 28 |
| Nitrogen - 500°C | 0.996 | 2.53 | 25 |
| Nitrogen - 550°C | 0.966 | 2.43 | 25 |
| Nitrogen - 600°C | 0.966 | 2.27 | 23 |



a) Ambient air



b) Nitrogen

Fig. 1. XRD patterns of $g-C_3N_4$ in a) ambient air and b) nitrogen atmosphere of samples synthesized at different temperatures

For the calculated interlayer distances (d_{002}) of samples, in the ambient air and nitrogen atmosphere, it was found that as temperature increased, these interlayer distances (d_{002}) tended to decrease. For the mean thickness of graphitic stack-based g-C₃N₄, the largest crystallites were obtained for g-C₃N₄ in the ambient air at 600°C with 5.52 nm and the smallest crystallites were g-C₃N₄ in nitrogen at 600°C with 2.27 nm. In the ambient air, higher temperature affected thicker graphitic stack-based g-C₃N₄ thickness and more layers of g-C₃N₄ due to higher crystallites. Conversely, in a nitrogen atmosphere, higher temperature affected thinner graphitic stack-based g-C₃N₄ thickness and less number of g-C₃N₄ layers.

The percent weight loss can be calculated using Eq. (4).

$$\%Weight\ loss = \frac{w_1 - w_2}{w_1} \times 100 \tag{4}$$

Where W_1 is the weight of urea before pyrolysis and W_2 is the weight of urea after pyrolysis. From Table 2, the weight loss percentage of urea synthesized in the ambient air was higher than that in nitrogen when compared at the same temperature. The weight loss percentage of urea increased as the temperature increased in the ambient air. The trend of weight loss percentage of urea synthesized in both nitrogen and ambient air atmosphere is shown in Fig. 2. It can be seen that the urea synthesized in the nitrogen atmosphere was similar at different temperatures while the weight loss percentage of urea in the ambient air atmosphere decreased significantly greater when the temperature elevated.

Table 2. The percent weight loss of urea in ambient air and nitrogen atmosphere samples synthesized at different temperatures

| | 450°C | | 500°C | | 550°C | | 600°C | |
|-----------------------|-------|----------------|-------|----------------|-------|----------------|-------|----------------|
| | air | N ₂ | air | N ₂ | air | N ₂ | air | N ₂ |
| % weight loss of urea | 94.31 | 95.67 | 95.75 | 94.87 | 97.87 | 94.75 | 98.74 | 96.21 |

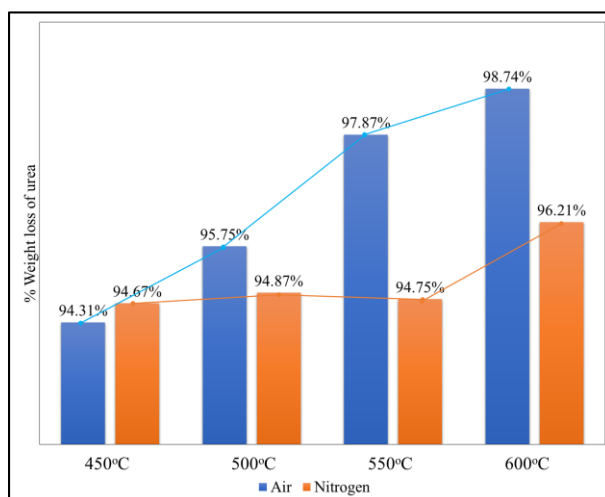


Fig. 2. Graph of weight loss percentage of urea in ambient air and nitrogen atmosphere

3.2 SEM analysis

The SEM image in Fig. 3. shows results of g-C₃N₄ synthesized in an ambient air and nitrogen atmosphere at different temperatures. These SEM images clearly show the structure of g-C₃N₄ consisting of stacked lamellar crystals that is consistent with the g-C₃N₄ that had been reported previously [12].

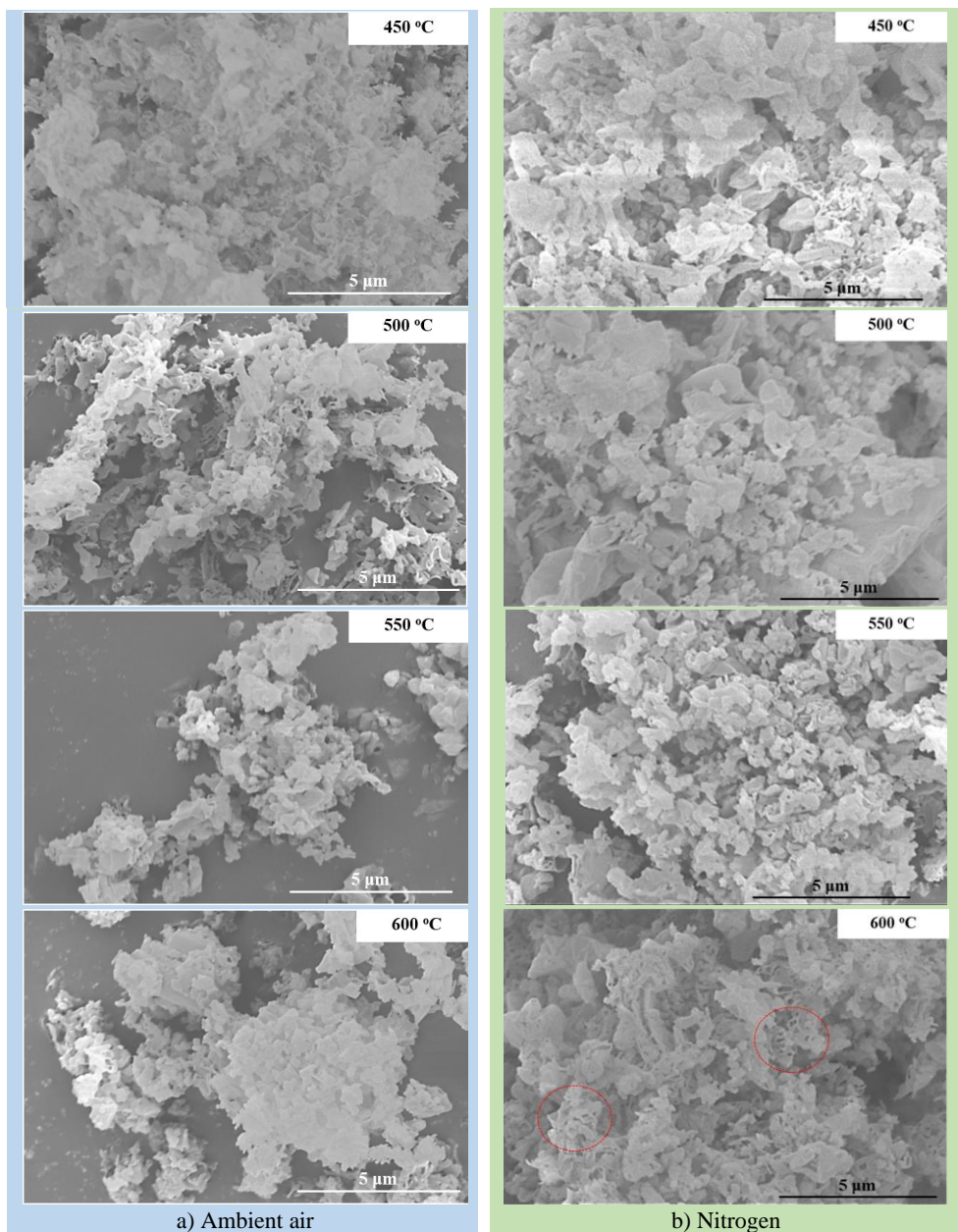


Fig. 3. SEM photograph of g-C₃N₄ in a) the ambient air and b) nitrogen atmosphere samples synthesized at different temperatures

However, a clear difference in g-C₃N₄ morphologies synthesized in the ambient air and nitrogen atmosphere at 600 °C was observed. In Fig. 3 a) the sample heated at 600°C in the ambient air was composed of a large stacked sheet. In Fig. 3 b), the sample heated at 600°C in nitrogen, a crystallized sheet was composed of a lot of small porous as circled in red. These small porous structures developed as a result of gas bubbles created during polymerization [15], [16]. In the ambient air, the morphologies of the samples at higher temperatures had an increasing specific surface area (BET surface area analysis) which were 44.34, 55.16, 44.54, and 121.9 m²/g at 450, 500, 550, and 600°C, respectively. The difference of specific surface areas of samples at 600°C in the ambient air was 121.9 m²/g and in nitrogen was 188.7 m²/g which provided a higher surface area.

3.3 Light absorption properties

The UV-Vis-NIR absorption spectra of g-C₃N₄ synthesized at different atmospheres and temperatures are shown in Fig. 4 a) and b). It showed that the optical absorption was red-shifted when the temperature was increased. The exception for the sample heated at 600°C in the ambient air which tends to be blue-shifted or wavelength decreases. The corresponding band gap energy (E_g) calculated using Tauc's equation is shown in Fig. 4 c). In the ambient air, the band gap energy of the samples heated at 450, 500, 550, and 600 °C were 2.97, 2.91, 2.87, and 2.92 eV respectively. While in the nitrogen atmosphere band gap energy of the samples heated at 450, 500, 550 and 600 °C were 2.95, 2.91, 2.92, and 2.85 eV respectively. One could observe that the sample annealed at 450 °C in the ambient air had the highest band gap energy while the sample heated at 600 °C in nitrogen had the lowest band gap energy. The band gap energy of g-C₃N₄ synthesized in nitrogen tended to be narrower than that synthesized in the ambient air.

Fig. 5. shows a comparison of band gap energy between g-C₃N₄ synthesized in the ambient atmosphere and nitrogen at different temperatures. It was shown that band gap energy in the nitrogen atmosphere tended to decrease with increasing temperature because of the amorphous structure formation [6]. In the ambient air, the band gap energy of the sample was lower with the higher temperature at 450 to 550 °C due to an amorphous structure (XRD analysis in Fig. 1.) and at 600°C, the band gap energy of the sample was increased with corresponding shorter wavelength range. Based on the results, the ambient air could be determined that pyrolysis of urea at 550°C was the optimized reaction temperature, which was similar to the previous report [10].

3.4 Photocatalyst property analysis

The photocatalytic efficiency of synthesized powders was evaluated by the degradation experiment of methylene blue solution under visible light irradiation (wavelength of more than 450 nm, generated from a 50 W LED lamp). After the suspension of photocatalysts in dark for 2 h and keeping record data for 15 and 30 min, the result as seen in Fig. 7. showed that the absorption spectra of solution of methylene blue exhibited slight change. This indicated the occurrence of the adsorption-desorption equilibrium. The photocatalytic activities of samples were shown in Fig. 6. After reacting for 7 h, samples prepared at higher temperatures tended to exhibit better performance. The g-C₃N₄ synthesized in the ambient air at 450, 500, 550, and 600°C achieved degradation efficiencies of 65.28%, 72.88%, 81.79%, and 95.50%, respectively. And the g-C₃N₄ synthesized in nitrogen at 450, 500, 550, and 600°C achieved degradation efficiencies of 67.65%, 74.48%, 78.06%, and 95.76%, respectively. The results also showed that the effect of temperature positively correlated to photocatalytic activity, higher temperature will increase photocatalytic activity efficiency. Based on the results, the samples heated at 600°C in both atmospheres had the superior photocatalytic activity

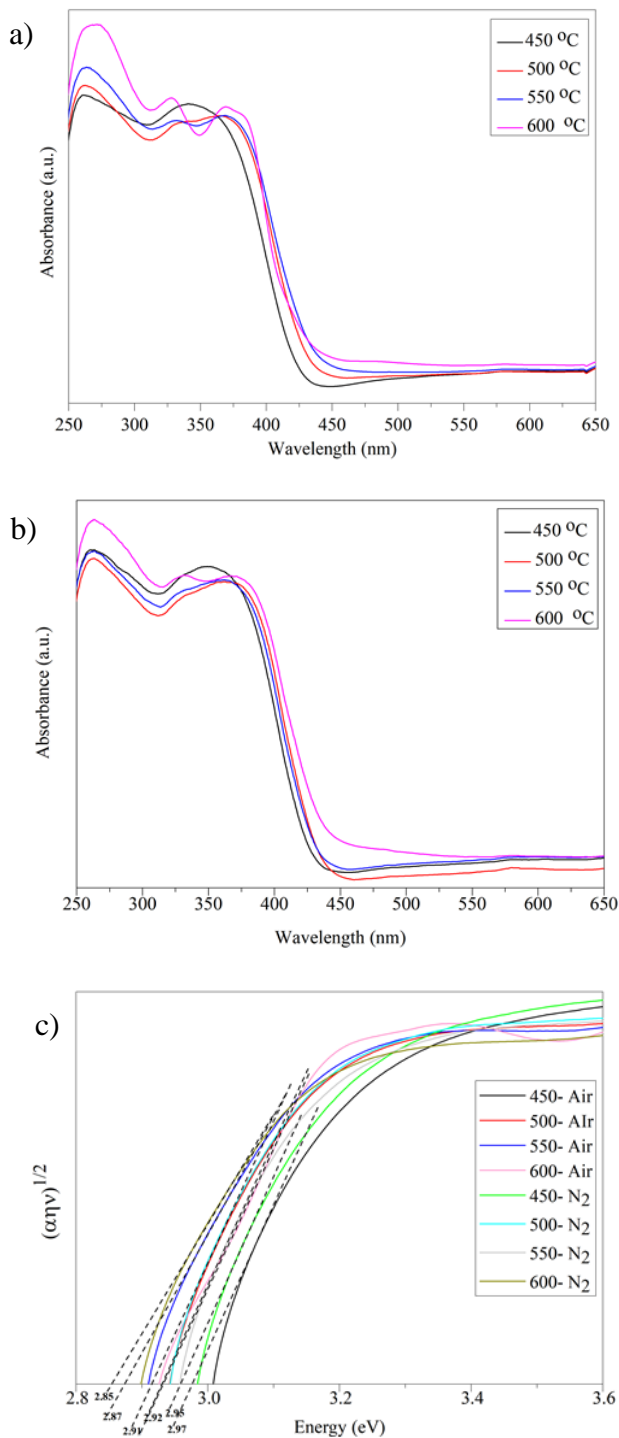


Fig. 4. UV-Vis-NIR spectra of g-C₃N₄ synthesized at different temperatures in a) ambient air and b) nitrogen atmosphere and c) determine the band gap energy of the g-C₃N₄ synthesized at different temperatures in the ambient air and nitrogen atmosphere by Tauc's equation plot.

efficiency as they both had the highest specific surface, which was a benefit for photocatalytic reaction. In the nitrogen atmosphere, band gap energy was reduced and effect to wavelength to absorb greater light energy. In the ambient air at 600°C, although band gap energy has a narrow range of wavelength but the highest crystalline results, in a good photocatalytic activity efficiency [1]. Moreover, the results also showed that the effect of temperature positively correlated to photocatalytic activity, higher temperature will increase photocatalytic activity efficiency.

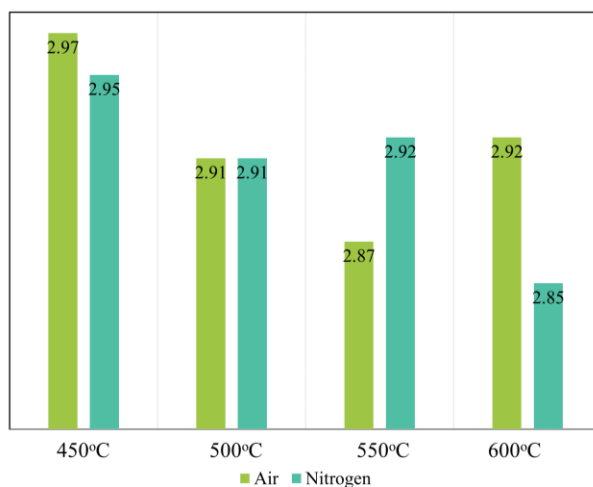


Fig. 5. The band gap energy (E_g) of the samples heated at different temperatures and atmospheres

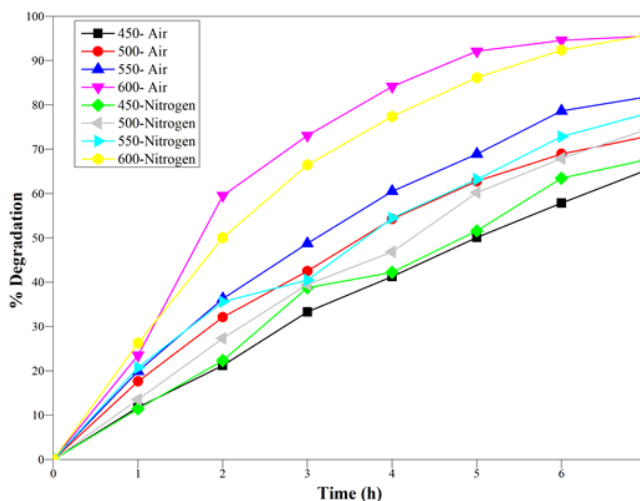


Fig. 6. Photocatalytic degradation efficiency as a function of time using g-C₃N₄ synthesized at different temperatures in ambient air and nitrogen atmosphere

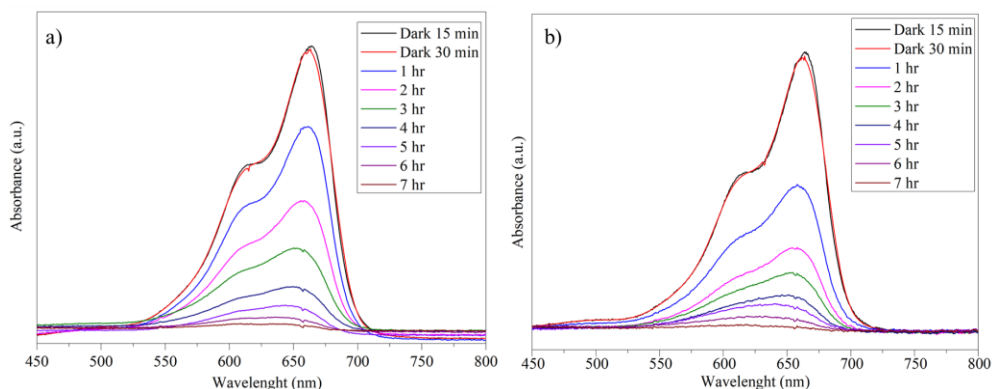


Fig. 7. Absorbance spectra of MB solution of the catalysts synthesized at 600°C in a) ambient air and b) nitrogen atmosphere.

4. Conclusion

The synthesized atmospheres and temperatures played an important role in the properties of the obtained g-C₃N₄. The crystal size was decreased by increasing temperature in the nitrogen atmosphere while increasing in the ambient air. The light absorption, at various temperatures and atmospheres, was not a significant difference but the band gap energy of g-C₃N₄ synthesized in nitrogen was narrower than that synthesized in the ambient air. The weight loss percentage of urea, in the ambient air, decreased greater than in nitrogen or the yield of products synthesized in the nitrogen atmosphere was higher than in the ambient air. Finally, the effect of temperature positively correlated to photocatalytic activity.

Acknowledgement

The project was supported by the department of materials science, Faculty of Science at Chulalongkorn University, and the Expert Centre of Innovative Materials, Thailand Institute of Scientific and Technological Research.

References

- [1] Wen J, Xie J, Chen X, Li X. A review on g-C₃N₄ -based photocatalysts. *Appl. Surf. Sci.* 2017;391:72-123.
- [2] Furukawa JY, Renata MM, Ana LM-J, Thalía SC-G, Vecxi JP-C, Catarina R, *et al.* Skin impacts from exposure to ultraviolet, visible, infrared, and artificial lights-a review, *J. Cosmet. Laser Ther.* 2021;23(1-2):1-7.
- [3] Zhang J, Sun H. 6 - Carbon nitride photocatalysts. In: Lin Z, Ye M, Wang M, editors. *Multifunctional photocatalytic materials for energy*: Woodhead Publishing; 2018. p. 103-26.
- [4] Li X, Yu J, Low J, Fang Y, Xiaoc J, Chen X. Engineering heterogeneous semiconductors for solar water splitting. *J. Mater. Chem. A* 2015;3:2485-534.
- [5] Niu P, Yin LC, Yang YQ, Liu G, Cheng HM. Increasing the visible light absorption of graphitic carbon nitride (melon) photocatalysts by homogeneous self-modification with nitrogen vacancies. *Adv. Mater.* 2014;26(47):8046-52.
- [6] Kang Y, Yang Y, Yin L-C, Kang X, Liu G, Cheng H-M. An amorphous carbon nitride photocatalyst with greatly extended visible-light-responsive range for photocatalytic hydrogen generation. *Adv. Mater.* 2015;27(31):4572-7.

-
- [7] Liang Q, Li Z, Huang ZH, Kang F, Yang QH. Holey graphitic carbon nitride nanosheets with carbon vacancies for highly improved photocatalytic hydrogen production. *Adv. Funct. Mater.* 2015;25(44):6885-92.
- [8] Yang P, Zhao J, Qiao W, Li L, Zhu Z. Ammonia-induced robust photocatalytic hydrogen evolution of graphitic carbon nitride. *Nanoscale* 2015;7(45):18887-90.
- [9] Jiménez-CP, Marchal C, Cottineau T, Caps V, Keller V. Influence of the gas atmosphere during the synthesis of g-C₃N₄ for enhanced photocatalytic H₂ production from water on Au/g-C₃N₄ composites. *J. Mater. Chem. A* 2019;7(24):14849-63.
- [10] Liu J, Zhang T, Wang Z, Dawson G, Chen W. Simple pyrolysis of urea into graphitic carbon nitride with recyclable adsorption and photocatalytic activity. *J. Mater. Chem.* 2011;21(38):14398-401.
- [11] Cao S, Low J, Yu J, Jaroniec M. Polymeric photocatalysts based on graphitic carbon nitride. *Adv. Mater.* 2015;27(13):2150-76.
- [12] Zheng Y, Zhang Z, Li C. A comparison of graphitic carbon nitrides synthesized from different precursors through pyrolysis. *J. Photochem. Photobiol., A* 2017;332:32-44.
- [13] Saner B, Okyay F, Yürüm Y. Utilization of multiple graphene layers in fuel cells. 1. An improved technique for the exfoliation of graphene-based nanosheets from graphite. *Fuel* 2010;89(8):1903-10.
- [14] Wang X, Maeda K, Thomas A, Takanabe K, Xin G, Carlsson JM, et al. A metal-free polymeric photocatalyst for hydrogen production from water under visible light. *Nat. Mater.* 2009;8:76-80.
- [15] Jiang D, Chen L, Zhu J, Chen M, Shi W, Xie J. Novel p-n heterojunction photocatalyst constructed by porous graphite-like C₃N₄ and nanostructured BiOI: facile synthesis and enhanced photocatalytic activity. *Dalton Trans.* 2013;42(44):15726-34.
- [16] Zhang Y, Liu J, Wu G, Chen W. Porous graphitic carbon nitride synthesized via direct polymerization of urea for efficient sunlight-driven photocatalytic hydrogen production. *Nanoscale* 2012;4(17):5300-3.